The American Journal of Human Genetics, Volume *98*

Supplemental Data

A Recurrent Mosaic Mutation in *SMO*, Encoding the Hedgehog Signal Transducer Smoothened, Is the Major Cause of Curry-Jones Syndrome

Stephen R.F. Twigg, Robert B. Hufnagel, Kerry A. Miller, Yan Zhou, Simon J. McGowan, John Taylor, Jude Craft, Jenny C. Taylor, Stephanie L. Santoro, Taosheng Huang, Robert J. Hopkin, Angela F. Brady, Jill Clayton-Smith, Carol L. Clericuzio, Dorothy K. Grange, Leopold Groesser, Christian Hafner, Denise Horn, I. Karen Temple, William B. Dobyns, Cynthia J. Curry, Marilyn C. Jones, and Andrew O.M. Wilkie

Supplemental Note: Clinical report

Subject 8

This female child was assessed at the age of 2 years. She had been born at 36 weeks' gestation to a 29 year old G3P2 mother and a 28 year old father. Fetal MRI was performed at 29 weeks' gestation because of occipital cystic swellings observed on a previous ultrasound scan. The MRI demonstrated facial abnormalities, abnormal right calvarial shape and frontal lobe sulcation, consistent with craniosynostosis, unilateral right microcephaly, and focal polymicrogyria. Occipital scalp lymphangiomas and bowel malrotation were also noted. At birth, she was noted to have facial asymmetry and duplicated syndactylous thumbs and halluces with variable syndactyly of digits 1-3 in all extremities. Dysmorphic features included scalp lymphangiomas, frontal bossing, flat nasal bridge, midface retrusion, prominent chin, and large ears. Postnatal brain MRI confirmed the prenatal findings, with the addition of cavum septum pellucidum with intact corpus callosum. Head computed tomography (CT) revealed extensive right coronal craniosynostosis, accessory bone at the anterior fontanelle, wormian bones of the left posterior skull, enlarged right lateral ventricle, and prominent extra-axial spaces. The scalp lymphangiomas were excised shortly after birth, and histologically described as hamartomatous lesions with features of lymphangioma and nevus sebaceus.

Early feeding difficulties prompted further investigation and bowel malrotation was discovered, requiring band division (Ladd's procedure) and ileostomy, which was later reversed. Serosal nodules noted in the duodenum, appendix, and mesentery were pathologically characterized as hamartomatous with fibrovascular and neuromuscular components. Subsequently, she has had extensive malabsorption, diarrhea, and intermittent pseudo-obstruction. Vesicoureteral reflux from birth caused frequent urinary tract infections. Although not present at birth, by 6 months of age linear areas of pigmentary mosaicism were evident over the extremities and trunk, while sparing the face and scalp; based on the failure to tan normally, the affected skin appeared to be the hypopigmented and atrophic component. Around 1.5 years of age, she was noted to have significant leg length discrepancy, left greater than right, and lumbar scoliosis. Her development has progressed well despite her complex problems, and she is walking, speaking in two word sentences, has pincer grasp, and is socially engaged. Currently, her height, weight, and head circumference are within the normal range.

Genetic testing results, including karyotype, SNP-based microarray, chromosome breakage studies, sequencing and deletion/duplication testing of *RECQL4*, *TWIST*, *FGFR1*, and *FGFR2*, selective mutational analysis of *FGFR3*, and clinical whole exome sequencing from blood-derived DNA did not indicate disease-causing mutations accounting for her phenotype.

Figure S1. *SMO* is the top hit in an analysis of variant allele frequency differences in two samples from Subject 1.

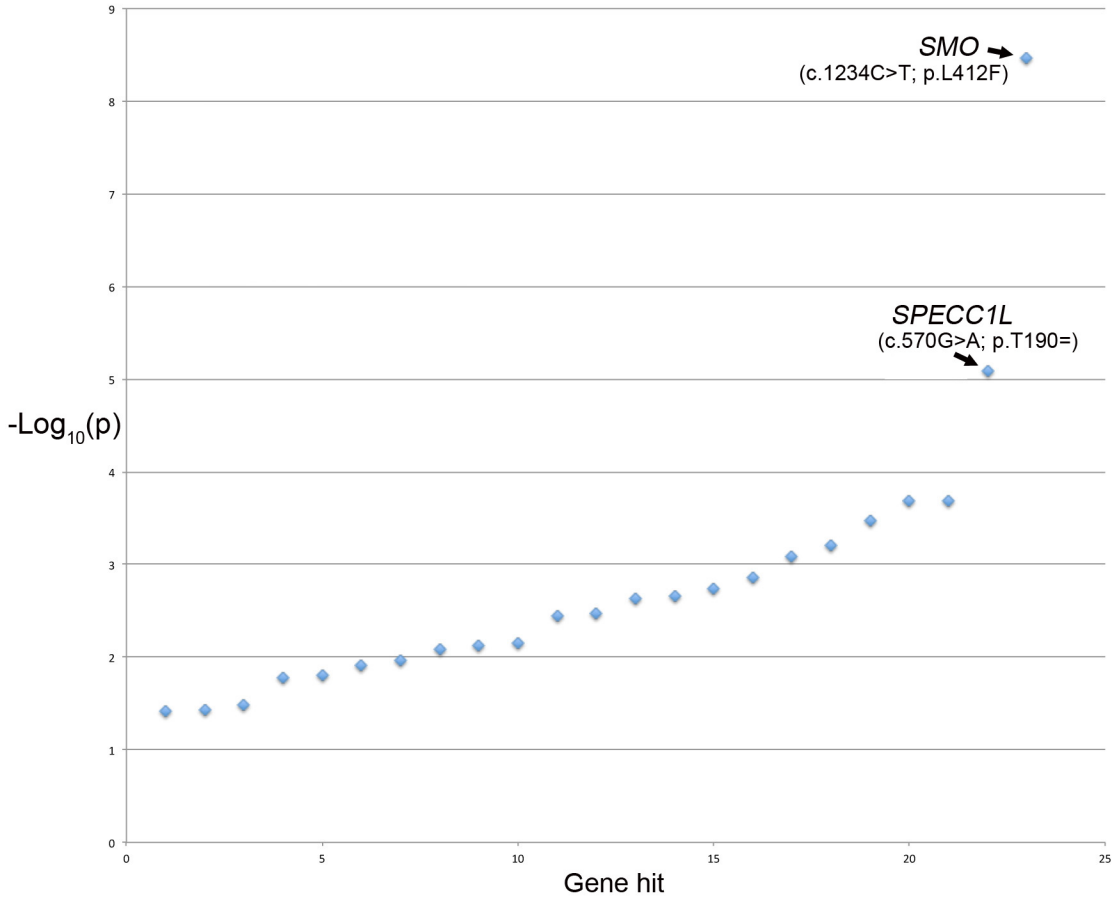

The exome data from Subject 1 (samples 1-2 and 1-4) was analysed using MiG (Multi-Image Genome viewer; McGowan et al., 2013). Only variants within exons and at positions with read depths greater than or equal to 20 were considered. A p-value threshold of 0.05 was used in the calling of somatic sites (threshold below which read count differences between two samples were deemed nominally significant). The variant frequency cutoff applied to the data was ≤15% in one tissue, and ≥30% in the other tissue, and vice versa. The 23 variant hits are shown plotted against $-\text{Log}_{10}(p)$.

Figure S2. Exome sequence of *SMO* exon 6 from Subject 2.

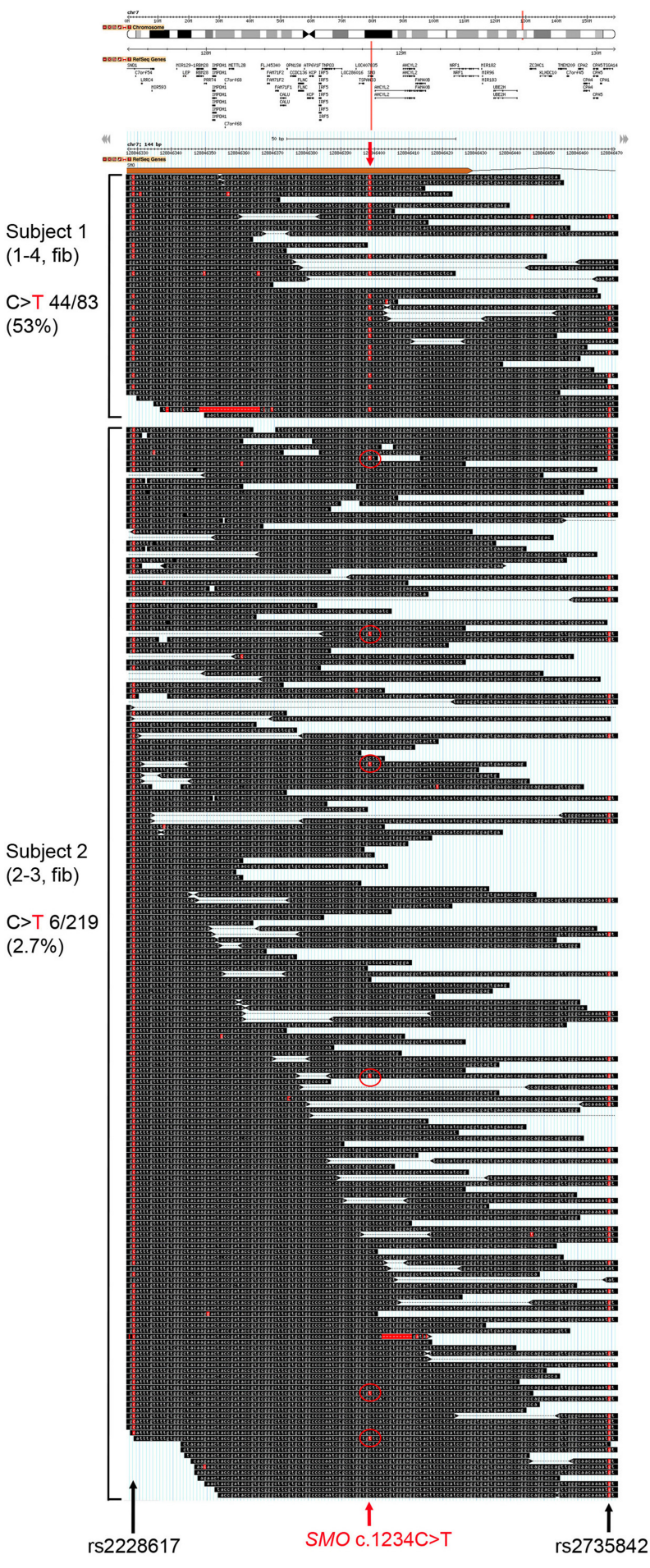

Exome sequencing reads, visualized in GBrowse, aligned to *SMO* exon 6 from Subject 1 (sample 1-4, not all reads are shown) shown above, and Subject 2 (sample 2-3), below. The red arrow indicates the 1234C>T mutation position. Mutant T reads in Subject 2 (6/219 reads) are circled for clarity and make up 2.7% of nucleotides at this position. The two flanking SNPs, rs2228617 upstream and rs2735842 downstream, are indicated by black arrows, and are both homozygous for the variant allele in Subject 2. The uppermost panel shows the position of *SMO*, and nearby genes, on chromosome 7q32.1.

Figure S3. Magnetic resonance imaging of brains of Subjects 5, 6 and 8.

Subject 5

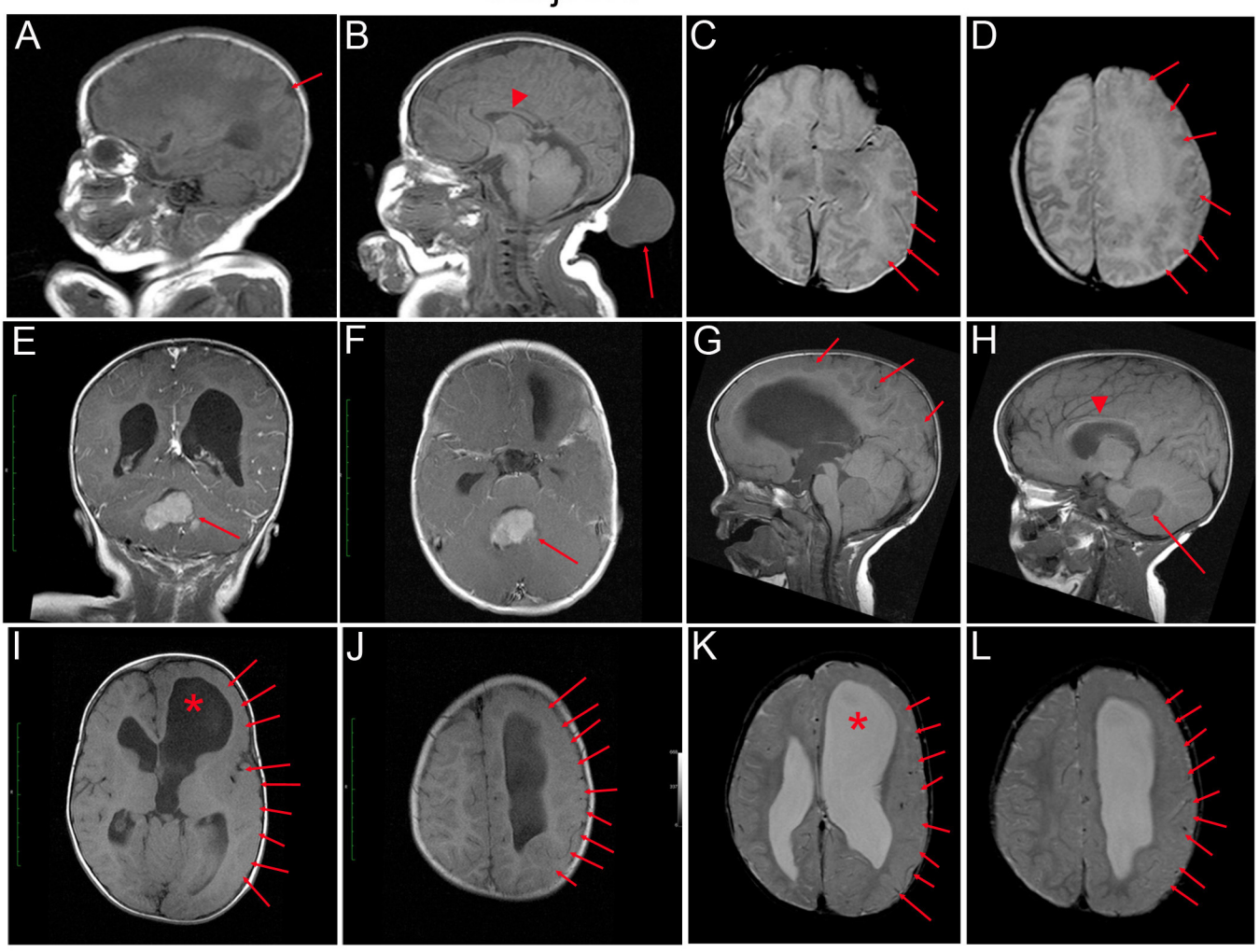

Subject 6

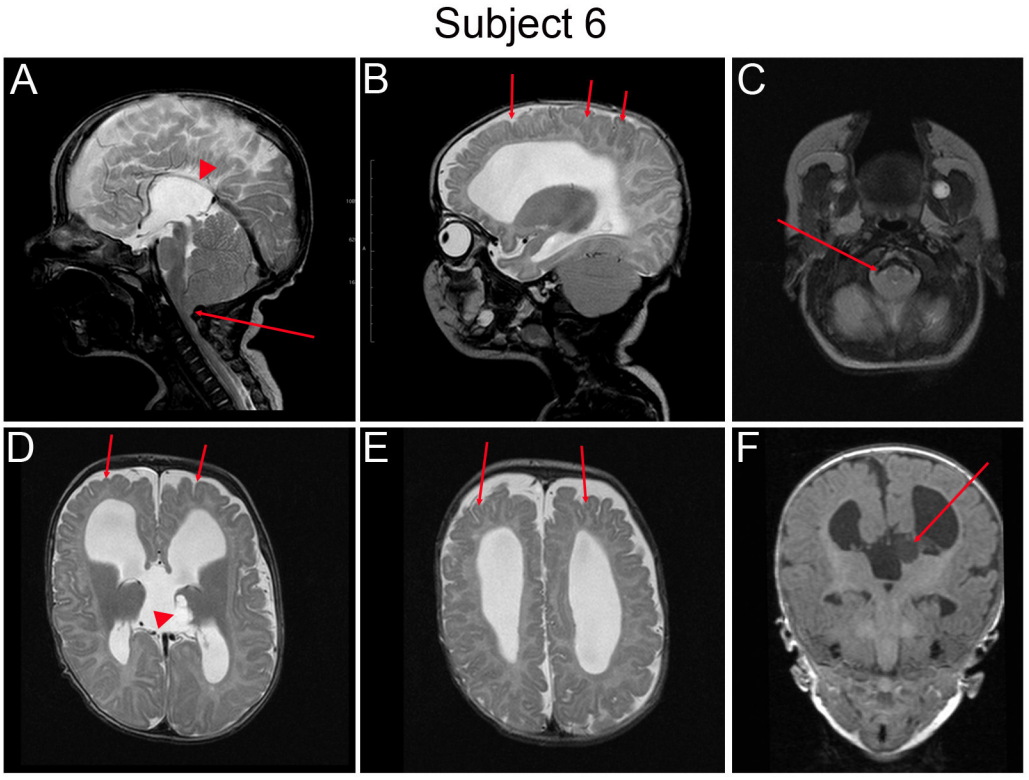

Subject 8

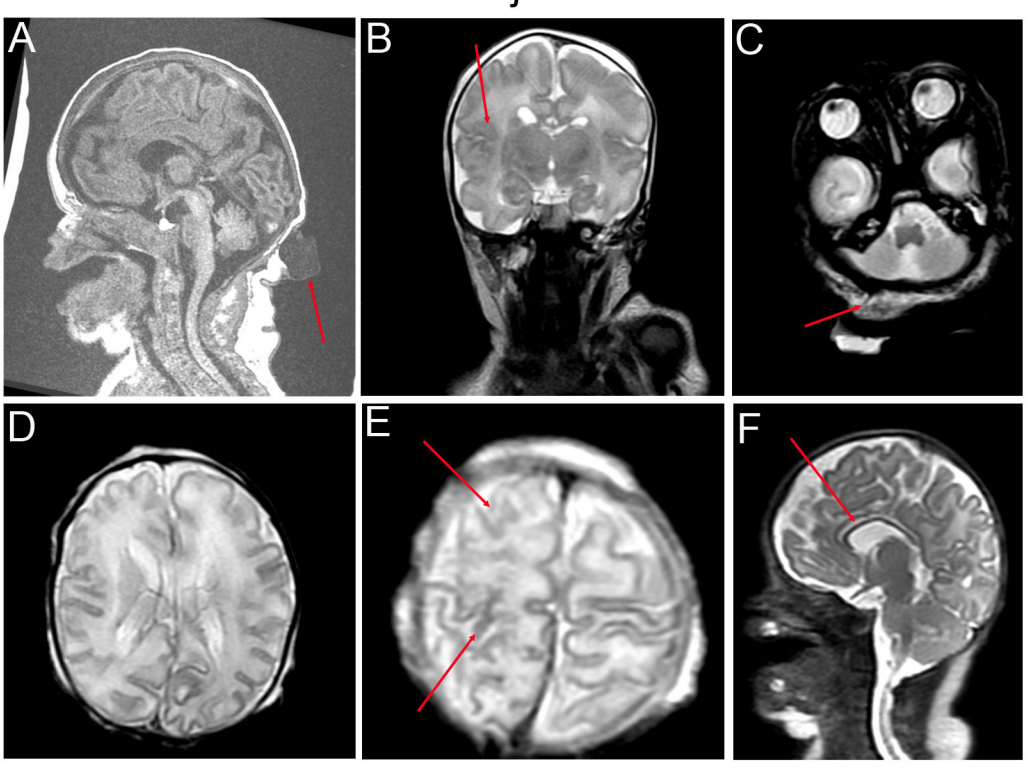

Top, brain MRI from Subject 5 aged 1 day (A-D) and 1 year 5 months (E-L). At 1 day the 4th ventricle is small and pinched with moderate cerebellar ectopia filling the low posterior fossa (B); in the second scan this has evolved to a more severe Chiari I malformation (G). In A and G note macrocephaly with prominent forehead and narrow extra-axial spaces. In B, the corpus callosum is shortened with absent rostrum and splenium consistent with partial agenesis (ACC, arrowhead, see also image H); note also a 3-4 cm occipital encephalocele connecting to the low posterior fossa (arrow, resected in the later set of images). In C,D,I-L note left hemimegalencephaly (HMEG) and ventriculomegaly (asterisks) with dysplastic cortex over part or all of the enlarged hemisphere with irregular gyral pattern and microgyri (arrows, also in A,G), consistent with polymicrogyria or classic HMEG. A single periventricular nodular heterotopia in the anterior-lateral body of the left lateral ventricle was also seen. In E and F, note large 2-3 cm contrast-enhancing tumour in the right cerebellar hemisphere and 4th ventricle (desmoplastic medulloblastoma also visible in H, arrows).

Middle, brain MRI from Subject 6 aged 3 months showing normal head size and extra axial spaces. In A, note very short and thin corpus callosum consistent with partial ACC (arrowhead), normal brainstem and cerebellar structures, but severe cerebellar tonsillar ectopia filling low posterior fossa and associated Chiari 1 malformation (arrow). In B there are small gyri, shallow sulci and subtle pebbling of cortex white matter border consistent with delicate polymicrogyria (arrows). C shows the cerebellar tonsils wrapped around low medulla (arrow). D, subtle abnormalities of gyri and cortex (arrows), cyst in left thalamus (arrowhead) that connects with 3rd ventricle-midline cyst. E, diffuse, small gyri and shallow sulci (most obvious in frontal lobes, arrows), with subtle pebbling of the cortex-white matter border. F, arrow indicates the cyst in the left thalamus.

Bottom, brain MRI from Subject 8 aged 1 day (A-E) and 19 days (F). A, note prominent forehead, turricephaly, hypoplastic cerebellum and occipital cyst (arrow). In B, simplified gyral pattern bilaterally and subtle cortex irregularity (indicated by the arrow in the right perisylvian region). C, base of the brain showing surface tissue thickening at position of lymphangiomatous malformation (arrow). D, mild hemisphere asymmetry (left>right) with too few gyri on both sides and subtle cortex irregularity. E, delicate polymicrogyria on right side only (arrows). F, thin corpus callosum (arrow) consistent with mild ACC, large 1 x 1.5 cm cavum septi pellucidi. The lymphangiomatous malformation has been resected.

Table S1 Genes for which rare coding variants were called in two of the samples analyzed by exome sequencing

Gene	Chr	Position	Reference			Variant			Function	Nucleotide and amino acid change	Sub-ject
				Reads			Reads				
				F	R		F	R			
CREBBP[a]	16	3779774	-	8	1	TCA	5	0	nonframeshift insertion	NM_004380; c.5271_5272insGAT:p.G1757_E1758insD	3
CREBBP	16	3828048	G	43	25	C	37	19	nonsynonymous SNV	NM_004380; c. 2077C>G:p.P693A	4
DNAH17[b]	17	76464741	T	53	25	C	50	24	synonymous SNV	NM_173628; c. 8763A>G:p.T2912=	4
DNAH17	17	76556949	C	1	9	T	1	5	nonsynonymous SNV	NM_173628; c. 1904G>A:p.C635Y	3
CRIPAK[c]	4	1388318	-	14	29	CACAC	9	21	frameshift insertion	artifact	4
CRIPAK	4	1388944	GTGGAGTGTT	3	1	ATGGAGTGCC	5	0	nonframeshift substitution	artifact	2

Note.— Filters: Exome Variant Server and 1000 genomes allele frequency ≤0.0001, no minimum deleterious score (for nonsynonymous substitutions), minimum variant read depth = 4, exclude variants from solved in-house data. We retained variants of all categories that were called in 25-75% of reads. This generated a final list of 1127 variants. The list shown here was generated after further filtering against the Exome Aggregation Consortium dataset (allele frequency ≤0.00001) and the 3 genes with coding variants shared by two cases are shown in the Table above. Platypus did not call *SMO* c.1234C>T in Subjects 2 and 3 owing to their very low frequencies.

[a]excluded because heterozygous loss-of function mutations cause Rubinstein-Taybi syndrome (MIM: 180849).

[b]excluded because one of the variants is synonymous.

[c]excluded because both the sequence changes are artifacts.

Table S2 Deep sequencing of *SMO* c.1234C>T in CJS samples – read depths and percentage mutant allele

Subject	Tissue sample			C allele	T allele	% T allele
	ID		Source[b]			
1*	1-1	2244	blood	3579	3	0.08
	1-2[a]	2245	eyelid	17507	2145	**10.9**
	1-3	6292	skin	3474	0	0
	1-4[a]	6291	fib (1-3)	1013	975	**49.0**
2*	2-1	1280	skin	24106	7827	**24.5**
	2-2	6736	skin	27755	9	0.03
	2-3[a]	3082	fib (2-1)	2650	109	**3.95**
	2-4	6737	fib (2-2)	14626	767	**4.98**
	2-5	6845	bowel[c]	40869	201	0.49
3*	3-1	6942	skin	38264	6040	**13.6**
	3-2[a]	2252	fib	6455	3	0.05
	3-3	6943	fib (3-1)	3940	12	0.30
	3-4	6640	saliva	2510	42	**1.65**
4	4-1[a]	5843	blood	2310	0	0
	4-2	6723	saliva	1850	2	0.11
5*	5-1	6628	blood	17577	6	0.03
	5-2	6629	saliva	39146	3000	**7.12**
	5-3	6702	meningocele[c]	15364	3806	**19.8**
	5-4	6703	medulloblastoma[c]	12745	9600	**43.0**
6*	6-1	6847	skin[c]	6306	952	**13.1**
6*	6-2	6838	saliva	19924	1137	**5.40**
	6-3	6862	abdominal tumor[c]	1711	993	**36.7**
	6-4	6867	abdominal tumor[c]	5295	2862	**35.1**
7*	7-1	7039A	skin	4224	150	**3.43**
	7-2	7039B	fib (7-1)	5181	193	**3.59**
	7-3	7038B	fib (7-5)	7844	2	0.03
	7-4	6802	saliva	5426	6	0.11
	7-5	7038A	bone marrow	4679	47	0.99
8*	8-1	6839	blood	21600	109	0.50
	8-2	6840	colon[c]	19853	1624	**7.56**
	8-3	6841	cecum[c]	20179	2042	**9.19**
	8-4	6843	bone[c]	859	0	0
	8-5	6842	thumb[c]	8233	0	0
9	9-1	6984	blood	13168	12	0.09
	9-2	7314	saliva	58987	24	0.04
10*	10-1	7634	skin	143303	71845	**33.4**
	10-2	7638	fib (10-1)	169197	32719	**16.2**
Control	11-1	6985	blood	5599	2	0.04
	11-2	6986	blood	3028	1	0.03
	11-3	7002	saliva	54728	6	0.01

[*]Mutation positive; Samples quantified as containing >1% of the c.1234T allele are denoted in bold; [a]Sample used in exome sequencing; [b]Tissue source of DNA, sample ID in brackets indicates the skin sample from which fibroblasts were cultured. DNA was extracted from peripheral blood, saliva and a minimum of three 10 µm FFPE sections using Nucleon BACC3, Oragene-DNA (DNA Genotek) and Qiagen DNA FFPE tissue kits, respectively. DNA from all other tissue was obtained by homogenization, followed by overnight proteinase K treatment, phenol-chloroform extraction and DNA precipitation. The starting tissue from which fibroblast (fib) cultures were derived is indicated in brackets. [c]FFPE samples.

Table S3. Primers and amplification conditions used for genetic analysis of *SMO*

Amplification of *SMO* exon 6 for dideoxy sequencing[a]

	Primer sequence 5′→3′		Product size (bp)
Amplicon	Forward	Reverse	
SMO exon 6	caggtggatggggactctgtgagtgg	ttcgtctgcctagagggtcaccttctact	285

Deep sequencing – 1st round amplification of *SMO*[b]

	Primer sequence 5′→3′		Product size (bp), not including tags
Amplicon	Forward (tag lowercase, gene-specific sequence uppercase)	Reverse (tag lowercase, gene-specific sequence uppercase)	
Exon 1-1	cgctcttccgatctctgGCTTTTGCTGAGTTGGCGG	tgctcttccgatctgacCCAGTCACCGCCGCGC	194
Exon 1-2	cgctcttccgatctctgGGCGGGAGCGCGAGGA	tgctcttccgatctgacACCAGAGCACGAGCTTGCCGT	196
Exon 1-3	cgctcttccgatctctgACTCGGACTCCCAGGAGGAAG	tgctcttccgatctgacGCACGTAACCTGCCCCCAAAG	204
Exon 2-1	cgctcttccgatctctgAGGTCTGACCAGTGATGGGCT	tgctcttccgatctgacACCCGGTCATTCTCACACTTG	200
Exon 2-2	cgctcttccgatctctgGATCCAGCCCCTGCTGTGTGC	tgctcttccgatctgacCAACCCAGAGAGCCTGGACC	215
Exon 3-1	cgctcttccgatctctgCGTCCCTGAGCTGCCTTGAC	tgctcttccgatctgacTGTAGCTGTGCATGTCCTGGT	210
Exon 3-2	cgctcttccgatctctgGCCAGAACCCGCTCTTCACAGA	tgctcttccgatctgacATCATGACCCTTCCCTGGGGA	211
Exon 4-1	cgctcttccgatctctgCAGGGAAGGGTCATGATCAGA	tgctcttccgatctgacCAATGCTGCCCACAAAGAAGC	193
Exon 4-2	cgctcttccgatctctgGAATCGCTACCCTGCTGTTATTCTC	tgctcttccgatctgacCACACTTCAGCCTTCCTCCCTG	198
Exon 5-1	cgctcttccgatctctgGAACCTCCAGACCTCAGCAGC	tgctcttccgatctgacCTTTGAAGGAAGTGTGCCAGGC	218
Exon 5-2	cgctcttccgatctctgGGTTTGGTTTGTGGTCCtcacc	tgctcttccgatctgacCCCCTCCCTCAAACTCACCC	208
Exon 6	cgctcttccgatctctgAGTAACCCACCTTCTGTCCCA	tgctcttccgatctgacCCAACTGGTCCTGGCCTGGT	191
Exon 7	cgctcttccgatctctgCTCACCCCTGCTAATGTCTGA	tgctcttccgatctgacGGTCGCATAGCCCCAGGA	206
Exon 8	cgctcttccgatctctgGACTCTCTCCTCCCCACTGCTG	tgctcttccgatctgacCCGCCTCCATGCCCCTCA	203
Exon 9-1	cgctcttccgatctctgTGGGTGACAGAGCAAGATCCT	tgctcttccgatctgacGTTCCAAACATGGCAAACAGGT	203
Exon 9-2	cgctcttccgatctctgGCCTTCTGGTGGAGAAGATCA	tgctcttccgatctgacTAGAGGCAGGACCCGACAAAA	201
Exon 10-1	cgctcttccgatctctgAGAGAAGGCCTCTACTCCTGAGTCC	tgctcttccgatctgacGGCAATCATCTTGCTCTTCTTGATC	206
Exon 10-2	cgctcttccgatctctgGCAGAGTGACGATGAGCCAAAG	tgctcttccgatctgacTGCCCCCAGCAGGCTGG	220
Exon 11	cgctcttccgatctctgGACCGGGAAGTCACTATTCCTTC	tgctcttccgatctgacCCCACCTTCCTCCAGAAGCT	217
Exon 12-1	cgctcttccgatctctgGCATGGACAGAGCCAGGGC	tgctcttccgatctgacGGTACTGGGGGCAGGGGCA	214
Exon 12-2	cgctcttccgatctctgCGCCTGGGCCGGAAGAAG	tgctcttccgatctgacGGGCTCTGGGCAGAATGGG	222
Exon 12-3	cgctcttccgatctctgGGGAGCTGGGGACTCTTGC	tgctcttccgatctgacCTCTTTCCTGTCCCAGGTCCTGC	240

Deep sequencing – 2nd round amplification of *SMO* fragments to incorporate barcodes and Ion Torrent PGM-specific primers[c]

	Primer sequence 5′→3′		Product size (bp)
	Forward (PGM-A sequence uppercase, 10 bp barcode, tag lowercase)	Reverse (PGM-P1 sequence uppercase, tag lowercase)	
Barcoding PCR	CCATCTCATCCCTGCGTGTCTCCGACTCAGxxxxxxxxxxcgctcttccgatctctg	CCTCTCTATGGGCAGTCGGTGATtgctcttccgatctgac	288-337

Note.—[a]DNA amplification was performed in a total volume of 20 µl containing 15 mM TrisHCl (pH 8.0), 50 mM KCl, 2.5 mM $MgCl_2$, 100 µM each dNTP, 0.4 µM primers, and 0.5 units of FastStart polymerase (Roche). Cycling conditions consisted of an 8 min denaturation step at 94°C, followed by 35 cycles of 94°C for 30 s, 68°C for 30 s and 72°C for 30s, with a final extension at 72°C for 10 min.
[b]The entire *SMO* coding region was amplified using tagged primers to generate products of approximately 200 bp (some exons required overlapping amplicons). Reactions used 0.02 U/µl of high fidelity Taq polymerase Q5 (NEB) in a volume of 25 µl containing, 40 ng DNA, 0.5 µM primers, 25 mM Tap-HCl (pH 9.3), 50 mM KCl, 2 mM $MgCl_2$, 1 mM ß-mercaptoethanol and 200 µM each dNTP. Cycling consisted of 30 s of denaturation at 98°C, followed by 15 cycles of 98°C for 10 s, 64°C for 20 s with a 0.5°C decrease each cycle and 72°C for 30s, and then a further 15 cycles of 98°C for 10 s, 57°C for 20 s and 72°C for 30s, with a final extension at 72°C for 2 min.
[c]Amplification products were diluted 1/100 and 2 µl used in a second round PCR, with a common reverse primer including the Ion Torrent PGM P1 adapter, and forward primers with Illumina 10 bp barcodes (to differentiate samples) and the Ion Torrent A adapter sequence. Reactions were set up as above in the first round PCR; cycling consisted of a 30 s denaturation step at 98°C, followed by 9 cycles of 98°C for 10 s, 60°C for 30 s and 72°C for 30s, with a final extension at 72°C for 2 min. Amplification products (roughly equal amounts as judged by EtBr staining in agarose gels) were combined and then purified with AMPure beads (Beckman Coulter). Emulsion PCR and enrichment was performed with the Ion PGM Template OT2 200 Kit (Life Technologies) according to the manufacturer's instructions. Sequencing of enriched templates was carried out on the Ion Torrent PGM (Life Technologies) for 125 cycles using the Ion PGM Sequencing 200 kit v2 and Ion 314 or 316 chips. Data were processed with Ion Torrent platform-specific pipeline software v4.2.1.

Table S4 Deep sequencing of *SMO* in trichoblastoma and nevus sebaceus (NS) samples

		SMO c.1234C>T			Analysis of entire *SMO* coding region			
	Sample	C allele	T allele	% T allele	Av reads all amplicons	Av base coverage	Min read depth	Variants with <1% minor allele frequency
Trichoblastoma	1	5257	2	0.04	2730	2042	217	
	2	3790	7	0.18	2244	1586	136	
	3	3819	20	0.52	1712	1182	83	
	4	3004	3	0.10	1463	1017	75	
	5	3334	6	0.18	1695	1106	142	rs201383344 (5′ end intron 3)
	6	201	1	0.50	998	595.9	48	
	7	3733	2	0.05	1376	982.3	99	
	8	4303	2	0.05	847	621.2	164	
	9	2433	3	0.12	1177	778.7	160	
	10	11237	9	0.08	4275	3098	645	rs201383344
	11	14904	7	0.05	1303	905.8	9	rs193242977; intronic homozygous G>A at 128,843,165 (hg19)
	12	2324	0	0	872	590.4	62	
	13	5206	16	0.31	1341	925.8	156	

	14	4394	3	0.07	1702	1177	177	
NS	1	3200	1	0.03	1653	1159	246	

Table S5 Comparison of brain imaging in Subjects 5, 6 and 8

	Subject 5	Subject 6	Subject 8
Brain malformation			
Occipitofrontal circumference	+3 SD	+4 SD	-0.2 SD
Cerebral asymmetry (or HMEG)	moderate	none	mild
Polymicrogyria (or FCD type 2)	+++	++	+
	L HMEG	PMG in FL	PMG R-PS
Ventriculomegaly (or hydrocephalus)	+	++	n
Agenesis of the corpus callosum	partial	partial	partial
Thalamic cyst	n	y	n
Meningocele	y	n	n
Chiari malformation type 1	y	y	n
Medulloblastoma in cerebellum and 4^{th} ventricle	y	n	n

Note.—abbrevations used: HMEG, hemimegalencephaly; FCD, focal cortical dysplasia; PMG, polymicrogyria; FL, frontal lobe; R-PS, right perisylvian region; y, yes; n, no.